Journal of Molecular Catalysis A: Chemical 333 (2010) 37–45

Contents lists available at ScienceDirect

Journal of Molecular Catalysis A: Chemical

journal homepage: www.elsevier.com/locate/molcata

The mechanism of the Fischer–Tropsch reaction over supported cobalt catalysts

Márton Kollár[a], Adriana De Stefanis[b], Hanna E. Solt[a], Magdolna R. Mihályi[a], József Valyon[a,*], Anthony A.G. Tomlinson[c]

[a] Institute of Nanochemistry and Catalysis, Chemical Research Center, Hungarian Academy of Sciences, Pusztaszeri út 59-67, Budapest 1025, Hungary
[b] Institute for Inorganic Methodologies and Plasma (IMIP)-CNR, Rome Research Area-CNR, Via Salaria Km 29,300, Monterotondo, (Rome) 00016, Italy
[c] Institute for the Structure of Matter (ISM)-CN, Rome Research Area-CNR, Via Salaria Km 29,300, Monterotondo, (Rome) 00016, Italy

ARTICLE INFO

Article history:
Received 4 May 2010
Received in revised form
17 September 2010
Accepted 18 September 2010
Available online 29 September 2010

Keywords:
Fischer–Tropsch mechanism
15%Co,0.5%Pt/γ-alumina
Co^{2+}-alumina-pillared clays
Operando DRIFTS

ABSTRACT

Natural gas and coal are converted to fuels by the Fischer–Tropsch reaction, i.e., by reacting CO with H_2, the currently accepted mechanism involving surface carbide formation. We have monitored the adsorbed species and their evolution during Fischer–Tropsch reaction on the commercial catalyst Pt,Co/γ-Al_2O_3 (as a standard), on Co/alumina-pillared montmorillonite (Co,Al-EFW) and its beidellite analogue (both are tri-octahedral smectite clays, but beidellite possesses tetrahedrally coordinated Al in the sheets) *via* optical diffuse reflectance (DRS[1]) and variable temperature *in situ* diffuse reflectance infrared Fourier transform spectroscopy (DRIFTS[2]). We show that in this case over Pt/Co-γ-Al_2O_3, under model conditions, H_2 reacts with CO forming H–C=O bridges over [Co-μO_2-Co] units; this transition state moiety also involves adjacent matrix Al–O–CO units. Subsequent stages provide differing oxygenate species *via* concerted acid–base reactions. The early stages of the Fischer–Tropsch synthesis thus do not involve surface carbide species and surface oxygenates are generated *via* concerted reaction of support surface Al-OH with the above HCO-bridging binuclear Co^{2+} unit.

1. Introduction

The search continues for cleaner and more efficient Fischer–Tropsch synthesis (FTS) reactions (i.e. hydrocarbon production from CO and H_2 on supported Co, Fe, Ru, or Mo often with added promoters) from syngas (CO/H_2) from natural gas or coal. Despite considerable work, the overall effects of support and porosity on FT reaction rate and hydrocarbon selectivities still remain unclear and reaction mechanism(s) controversial, even for commercial-type catalysts (e.g. 15%Co,0.5%Pt/γ-Al_2O_3) [1]. Over the years, mechanisms have veered from the original oxygenate mechanism extant until the 1970s to the current surface carbide mechanism [2]. Even defining the active sites, a necessary pre-requisite for defining mechanisms, has proved a daunting task, although iron and cobalt-based catalysts probably have different active sites. Further, the effect of promoters is complex and presumably steers the reaction [3]. Despite these difficulties, efforts to find superior catalysts continue, especially due to growing interest in FTS under supercritical conditions [4] to ensure isothermal conditions for this exothermic reaction, liquid like solubility and favourable diffusion. Clarification can come about only as a result of plausible mechanism(s) for the reaction being put forward from *in situ* (or '*operando*') experiments.

As regards cobalt, indications exist from the early FTS literature that reducibility of Co species on oxide supports depends both on the nature of the support and the Co distribution between differing supported phases (crystalline Co_3O_4, 'cobalt silicate', etc.). However, only relatively recently is structural definition being attained. For example, *via* EXAFS[3] and *in situ* XRD for Co/SiO_2, Khodakov et al. [5] found that calcination of oxidised Co catalyst under inert atmosphere results in a selective transformation of Co_3O_4 to CoO at 350–400 °C. FT-IR with CO as a molecular probe revealed that after H_2 reduction at 723 K, Co is present at different sites: Co metal sites (ν_{CO} = 2025 cm^{-1}), Co^{2+} ions in the crystalline phase of CoO (ν_{CO} = 2143 cm^{-1}) and Co^{n+} species in the amorphous phase (ν_{CO} = 2181 cm^{-1}). The authors concluded that the hydrogen reduction properties of the supported cobalt oxide particles depend on the Co_3O_4 crystallite size. Studying carbon-supported cobalt catalysts the FT activity was found to be structure sensitive [6]. The particle-size effect appeared in combination with CO-induced surface reconstruction of the Co metal particles. The structure of the active atomic ensemble remained undefined. The active site determination for Pt promotion of Co/γ-Al_2O_3 reduction (important for

* Corresponding author. Tel.: +36 1 438 1132; fax: +36 438 1164.
E-mail address: valyon@chemres.hu (J. Valyon).
[1] Optical diffuse reflectance spectroscopy.
[2] Diffuse reflectance infrared Fourier transformation spectroscopy.
[3] Extended X-ray absorption fine structure.

1381-1169/$ – see front matter © 2010 Elsevier B.V. All rights reserved.
doi:10.1016/j.molcata.2010.09.014

eventually identifying the mechanism on 15%Co,0.5%Pt/γ-Al_2O_3 of relevance here) is more advanced. From *in situ* EXAFS (Co *K* and Pt *LIII* edges) Jacobs et al. [7] concluded that: (i) isolated Pt atoms interact with supported cobalt clusters without forming observable Pt–Pt bonds, and (ii) cobalt cluster size increases slightly on Pt promotion. Further, XANES[4] showed that the cobalt clusters remaining after the first stage of TPR[5] are almost entirely cobalt (II) oxide. After the second stage of TPR, the residual oxide persisting in the sample is Co(II)aluminate (as confirmed by XPS).

In the interim, periodic MTS[6] model supports, such as MCM-41, SBA-15, and pillared clays have joined the FTS catalyst portfolio. As regards PILCs[7], Barrault et al. [8] reported some time ago that Fe-doped pillared laponites act as selective catalysts for the conversion of syngas into light hydrocarbons even at high temperature (700 K). (Laponite is a synthetic hectorite). We are extending this to newer supports (such as in Ref. [9]). In order to obtain molecular-level information on the nature of the adsorbed species and their respective evolution during the FTS reaction, it is important to explore reactants, products and possible intermediates simultaneously on the working catalyst. A well-tested technique for this application is *in situ* DRIFTS–MS[8] in which a special IR cell acts as a reactor and its downstream flow is analysed by a coupled on-line detection device (MS).

We here report a DRS/*in situ* DRIFTS study of Co(II)-exchanged alumina-pillared montmorillonite ('Co,Al-EFW') and its Co/Al-beidellite analogue ('Co,Al-B4'), and compare them with a commercial-type 15%Co/0.5%Pt/γ-Al_2O_3 catalyst.

2. Experimental

2.1. Materials

γ-Al_2O_3 was synthesized as described in Ref. [10] 15%Co,0.5%Pt/γ-Al_2O_3 was prepared from γ-Al_2O_3 using Co(II)-acetate, K_2PtCl_4 salts and incipient wetness impregnation technique.

Co,Al-EFW (Al/Co = 1) and Co,Al-B4 (Al/Co = 10) are cobalt-alumina-pillared montmorillonite (starting material from IKO-Erbslöh, Germany) and beidellite ('B4', S&B Minerals, Greece), respectively, described in detail in Ref. [9]. Co/Al-pillared clays were prepared using the appropriate metal-chlorides ($AlCl_3$, Carlo Erba; $CoCl_2$, Fluka). The metal-chloride solution (100 ml, 0.2 M $AlCl_3$ and 0.02 M $CoCl_3$, Al/Co = 10 or 0.2 M $AlCl_3$ and 0.2 M $CoCl_3$, Al/Co = 1) were mixed drop-wise (under stirring) with 0.2 M NaOH (Fluka) solution, which leads to the clear pillaring solution. The latter was then added drop-wise to the stirred colloidal clay solution (5 g clay in 500 cm^3 water). The excess salt contents of the pillared clays were removed with 'Visking' dialysis membranes. The chloride-free materials were than calcined at 723 K for 2 h in air. Co,Al-EFW and Co,Al-B4 were impregnated with Co and Pt salts (Co(II)-acetate, K_2PtCl_4) using the standard incipient wetness impregnation technique to obtain samples Co,Pt/Co,Al-EFW and Co,Pt/Co,Al-B4.

2.2. Physical measurements

XRD patterns were recorded on a Philips PW 1810 powder diffractometer, equipped with a graphite monochromator, using CuK_α radiation. Optical spectra, as diffuse reflectance (DRS) were collected at room temperature and after calcination at 400 °C before and after metal ion-loadings on a Cary 5 UV–vis–NIR Spectrophotometer against $BaSO_4$ as reference.

2.3. In situ DRIFTS–MS experiments

Spectral analysis of the catalyst surface during CO adsorption/catalysis was carried out using a Nicolet 5PC spectrometer equipped with a COLLECTOR™ II diffuse reflectance mirror system and a high-temperature/high-pressure DRIFTS reactor cell (Spectra-Tech, Inc.) as described in detail elsewhere [11]. The reactor cell was connected to a quadrupole mass spectrometer (MS) for real-time MS analysis of the DRIFTS reactor effluent. The sample cup of the cell was filled with 15–30 mg of powdered sample. Prior to each run, catalyst samples were pre-treated *in situ* as follows.

Pre-treatment in a dried 10% O_2/He stream; flow rate: 30 cm^3/min, Temperature programme: the sample was heated at a rate of 10 °C/min from 30 °C to 350 °C then held at 350 °C 60 for minutes. At 350 °C flushing with dried He for 10 min, then cooling to 320 °C in He. Reduction in dried 100% H_2 at 320 °C for 105 min, then at 350 °C flushing with dried He for 5 min.

Spectra were recorded at 30 °C, 100 °C, 200 °C, 240 °C, 280 °C in He, 3% CO/He, and in 33% CO/2% Ar (as reference)/65% H_2. The flow rate was 15 cm^3/min. The experimental setup parameters were: scan number: 256, resolution: 2 cm^{-1}. Three spectra were taken at each temperature first in He after pre-treatment (background) then in the presence of the gas mixture and, finally after 5 min flushing of the gas mixture by He.

In each case the background was subtracted from the spectra of the catalyst and the adsorbed surface species. The gas phase spectrum of the CO/He and CO/H_2 streams was taken over KBr at each temperature. This spectrum was used to correct the spectra for the gas phase CO. All DRIFTS experiments were carried out under atmospheric pressure.

Using the DRIFTS–MS system the FT activity was tested in the 280–320 °C temperature and the 1–10 bar pressure range. The MS was monitoring the ions with *m/z* ratio 2 and 28 to get information about the CO and H_2 conversion, respectively. Since CO and water give MS signal at *m/z* = 16, the methane yield was calculated from the intensity of the *m/z* = 15 peak. The peak intensities were not corrected for the possible but small interference of fragments from product hydrocarbons. The appearance of MS peaks at *m/z* = 27, 44 and 57 indicated the presence of hydrocarbons in the reactor effluent.

3. Results and discussion

3.1. DRS evidence for Co–O–Co units

The materials investigated are listed in Table 1 together with their porosity characteristics; XRPD[9] and DRS patterns are shown in supplementary Figs. 1 and 2.

The first point of note is that none of the materials gives DRS showing bands at 670 nm and 1400 nm characteristic of Co_3O_4 [12]. Instead, after calcination at 400 °C the DRS of all three catalysts show bands due to *d–d* transitions in the NIR[10]/visible region. For 15%Co,0.5%Pt/γ-alumina three split bands assignable to $^4T_1(F) \leftarrow {}^4A_2$ (4330 and 4560 cm^{-1}), $^4T_1(F) \leftarrow {}^4A_2$ (6700, 7600, 8150 cm^{-1}) and $^4T_1(P) \leftarrow {}^4A_2$ (15,000, 16,300, 17,200 cm^{-1}) are visible, as expected for presence of a pseudo-*Td* [CoO_4] moiety [13]. Co,Al-EFW and the beidellite analogue show bands in the same regions, also assignable to pseudo-*Td* [CoO_4] moieties. The

[4] X-ray absorption near-edge structure.
[5] Temperature-programmed reduction.
[6] Micelle-Templated silica.
[7] Pillared interlayered clays.
[8] Diffuse reflectance infrared Fourier transformation spectroscopy coupled with mass spectrometry.
[9] X-ray powder diffraction.
[10] Near infrared.

Table 1
Catalyst characteristics.

Material	Specific surface area (m^2/g)	Pore volume (cm^3/g)	Material	Cobalt content (wt%)	Platinum content (wt%)
γ-Al_2O_3	225	0.53	Co,Pt/γ-Al_2O_3	15	0.5
Co,Al-EFW	64.6	0.05	Co,Pt/Co,Al-EFW	13	0.1
Co,Al-B4	178	0.11	Co,Pt/Co,Al-B4	11.3	0.1

Table 2
Conversion of 33% CO/2% Ar/65% H_2 gas mixture.[a]

Catalyst	SV for CO[b], μmol s^{-1} g_{cat}^{-1}	t, °C/p, bar	CO, conv.[c], %	H_2, conv.[c], %	CH_4, yield[d], %	H_2/CO, conv. ratio	m/z diagnostic for C_2–C_4 products[e]
Co,Pt/γ-Al_2O_3	88	280/1	~4	~4	0.7	–	27, 30, 44, 57
Co,Pt/γ-Al_2O_3	88	280/10	25.6	31.1	4.1	2.4	27, 30, 44, 57
Co,Pt/γ-Al_2O_3	177	320/10	31.9	35.7	8.8	2.2	27, 30, 44, 57
Co,Pt/Co,Al-EFW	109	280/1	~2	~2	0.5	–	–
Co,Pt/Co,Al-EFW	77	300/10	17.6	22.0	7.6	2.5	27, 30, 44, 57
Co,Pt/Co,Al-EFW	77	320/10	25.7	35.5	13.2	2.7	27, 30, 44, 57

[a] Measured by the DRIFTS–MS system after about 30–60 min TOS.
[b] Space velocity.
[c] The CO and the H_2 conversions were determined from m/z = 28 and 2 MS peaks, respectively. The peak intensities were not corrected for the possible interferences with hydrocarbon fragments.
[d] The methane yield was estimated from the intensity of the MS peak at m/z = 15.
[e] The of given MS peaks were evidencing the formation of C_2–C_4 hydrocarbons.

evidence for M^{2+} bonding in alumina-PILCs has to date been overwhelmingly in favour of coordination to alumina pillar (rather than aluminosilicate sheet) [14]. More importantly, the DRS of all three also show bands in the 33,333–20,000 cm^{-1} region – not assignable to higher energy matrix charge-transfer bands, which occur at ca. 47,000 cm^{-1} for alumina [15]. Evidence is accumulating that bands in this region are due to MMCT[11] transitions [16]. Thus, the band at 21,100 cm^{-1} (with an ill-defined high-energy shoulder) in Co,Al-EFW may be assigned to a Co–Co MMCT, as also those at 24,500 cm^{-1} with shoulder at ca. 25,200 cm^{-1} in the beidellite analogue. Following the arguments of Ref. [17], this implies the presence of dimeric Co–O–Co (or more probably Co-μO_2-Co) units. 15%Co,0.5%Pt/γ-alumina also shows a band in this region, at 25,000 cm^{-1}, although this is partially masked by an intense further absorption consisting of at least five bands at ca 24,000, 26,000, 28,000, 32,000 and 37,000 cm^{-1}. The platinum was delivered from a $[PtCl_6]^{4-}$ solution; for ZSM-5 this gives rise to a well-characterised $[Pt_6]$ cluster [18] with optical spectra having bands in the same region.

3.2. Conversion in the DRIFTS–MS reactor

Conversion of CO/H_2 mixture to hydrocarbons was observed over the studied catalysts under the applied DRIFTS–MS conditions (Table 2). At low conversions methane was the only hydrocarbon product. Higher conversions and higher hydrocarbons were obtained at higher pressures.

3.3. DRIFTS identification of the surface species

Turning to the DRIFTS spectra, these will be treated under those for the bonded CO region (1800–2200 cm^{-1}), bonding hydrocarbon region (2700–3200 cm^{-1}) and bonding oxygenate species region (1200–1700 cm^{-1}). CO adsorption, particularly on basic oxide supports such as alumina, gives rise to various formate, carboxylate and carbonate species [19] with diagnostic bands in the 1200–1600 cm^{-1} region. The latter are often seen as 'spectator' species (i.e. coincidental to the major surface mechanism(s)) we show below that this is not the case here and differing oxygenates provide clues as to preferred reaction paths. Finally, we recall that TPD (temperature programmed desorption) studies have shown that apart from the alumina support itself, the Co/γ-alumina catalyst contains three phases: (i) a $CoAl_2O_4$ spinel phase, (ii) an amorphous or microcrystalline Co_3O_4 phase interacting with the support, and (iii) a crystalline Co_3O_4 phase [20–22]. The Co^{2+} ions of the spinel phase are rather inactive to CO adsorption; this is usually ascribed to their tetrahedral coordination and surface shielding [23]. Less is known of the surface structure of alumina pillars in PILCs, structural characterisation being notoriously difficult for this class of materials [24] although MAS NMR point to a γ-alumina (or close to γ-alumina) type surface [25]. The structural effect of substituting M^{2+} cations (here Co^{2+}) is also unclear. However, from MAS NMR studies it is known that Ga^{3+} and Cr^{3+} isomorphously substitute into the Al_{13} Keggin-ion precursor, whereas Fe^{3+} does not, because Al^{3+} present in solution catalyse the formation of polyhydroxyoxo-Fe^{3+} species [26,27]. The latter then decorate the final alumina pillar, which we recently showed to have important consequences for de-NO_x reactions [28].

3.3.1. Bonded CO region

Several bands in the 1980–2100 cm^{-1} region are usually observed for both mononuclear and polynuclear cobalt polycarbonyls and are assigned to linear carbonyl stretching modes. Busca et al. [29] analysed the well-resolved such spectra in the FT-IR of CO adsorbed on Co_3O_4 after reduction with H_2 in detail. In addition, bands at frequencies as low as 1900–1700 cm^{-1} can also appear for: (i) cobalt polycarbonyl clusters, associated with the presence of μ_2 or μ_3-bridging carbonyls, and (ii) negatively charged cobalt polycarbonyls [29]. More extensive is the study of a 12%Co/γ-Al_2O_3 by Rygh and Nielsen [30], which uses semiempirical (ASED-MO[12]) calculations as a guide for assigning CO vibrational modes.

The major general points of note for the DRIFTS spectra of Figs. 1 and 2 are: (i) CO adsorption begins at room temperature, and (ii) the spectra are very different between the two catalyst classes. Taking 15%Co,0.5%Pt/γ-Al_2O_3 first, at 30 °C there are two major CO bands attributable to ν(CO) stretches of Co–CO at 2158 cm^{-1} and 2042 cm^{-1} (Fig. 1B). The former is already no longer present at 200 °C and from 200 °C the latter is transformed into a broad

[11] Metal to metal charge transfer.

[12] Atom superposition and electron delocalization molecular orbital theory.

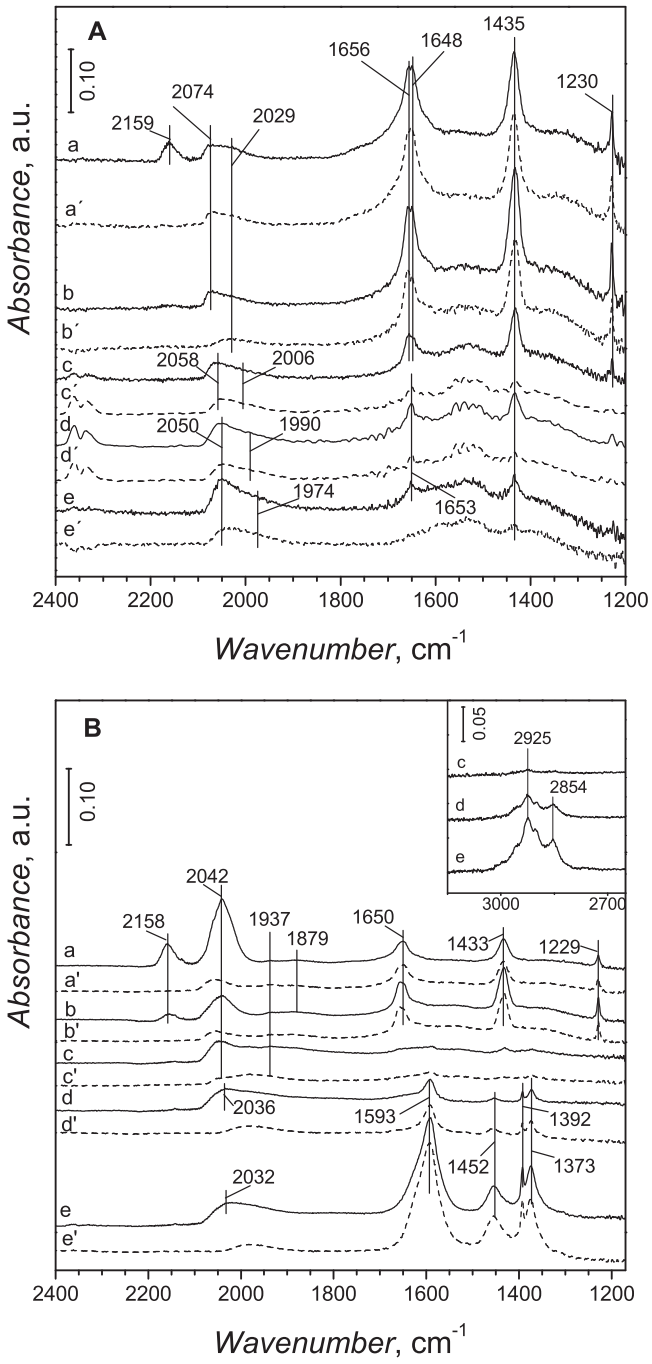

Fig. 1. *In situ* DRIFTS of 15%Co,0,5%Pt/γ-Al_2O_3. (A) Under 3%CO/He; (B) under 33%CO/H_2. a, b, c, d, e in 3% CO/He or in 33% CO/H_2 at 30 °C, 100 °C, 200 °C, 240 °C, 280 °C, respectively. a′, b′, c′, d′, e′ flushed with helium at 30 °C, 100 °C, 200 °C, 240 °C, 280 °C, respectively. (Standard DRIFTS conditions and designations). Inset: enlarged portions of spectra c, d and e.

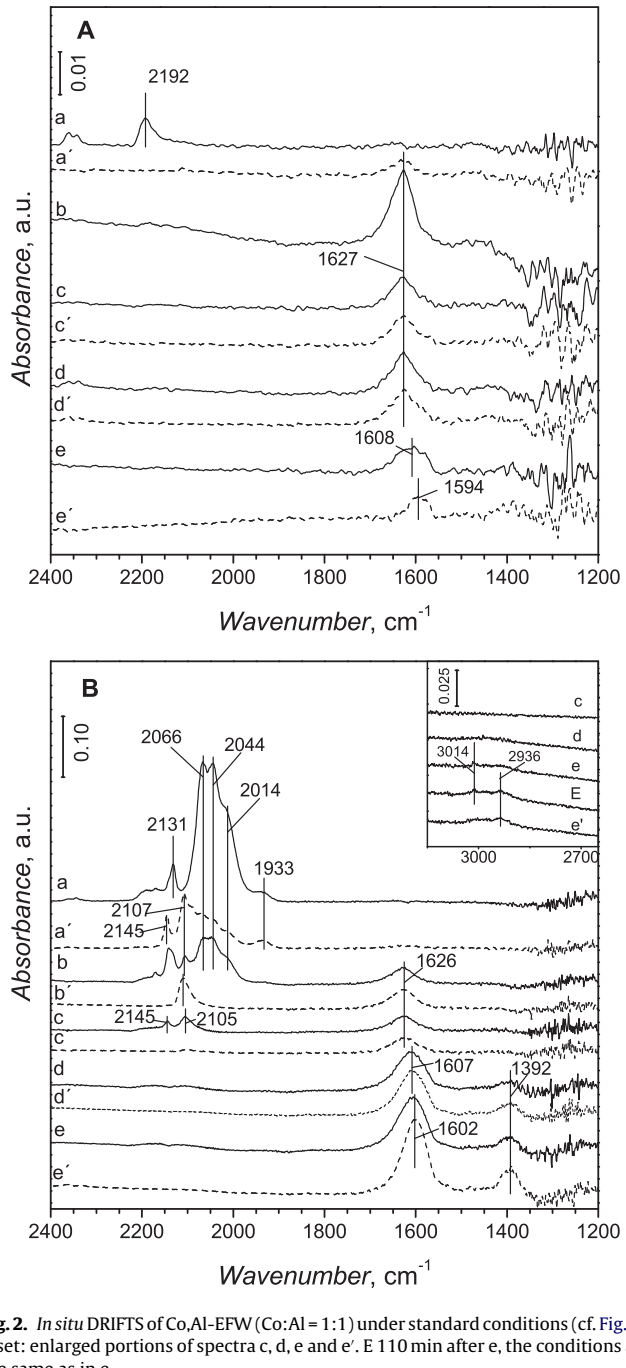

Fig. 2. *In situ* DRIFTS of Co,Al-EFW (Co:Al = 1:1) under standard conditions (cf. Fig. 1). Inset: enlarged portions of spectra c, d, e and e′. E 110 min after e, the conditions are the same as in e.

band at 2040 cm^{-1}, with one (or possibly two) weak shoulders to lower frequencies. In agreement with others [31] the 2042 cm^{-1} band is assigned to linearly adsorbed CO. As in Ref. [32], we ascribe the intensity decrease with simultaneous slight frequency shift on increasing the temperature as an indication of decreasing CO coverage as reaction proceeds. However, there is also evidence for two weak bands <1950 cm^{-1} (at 1937 and 1879 cm^{-1}, see Fig. 1B) the region usually associated with bridging CO [32,33] and we suggest that it arises from CO bridging the dimeric Co-μO_2-Co unit inferred from the DRS above. Differently than reported in Ref. [31], where a doublet in this region (also ascribed to bridging CO) disappears at 200 °C, the weak band here persists until 200 °C. We presume this is due to slight differences in conditions; Fredriksen et al. [32] suggest that coking preferentially removes active sites for bridging CO; presumably it is lower on our samples.

Conversely, the band at 2074 cm^{-1} which shifts to 2050 cm^{-1} as the temperature is raised to 280 °C can be ascribed to CO adsorption on Pt^0 sites (Fig. 1A) [34].

In contrast, at low CO flow concentration Co,Al-EFW (i.e. with no Pt promoter) gives a rather featureless DRIFTS, only a single band easily removed on flushing (even at 30 °C) appearing at 2192 cm^{-1} assignable to linearly coordinated CO (Fig. 2A). As expected, higher CO/H_2 reaction leads to a much richer carbonyl region, which shows 6 bands, all of which progressively disappear between 30 and 200 °C. Following the correlations of Busca described above [29], and noting the absence of vibrations characteristic of μ_2- or

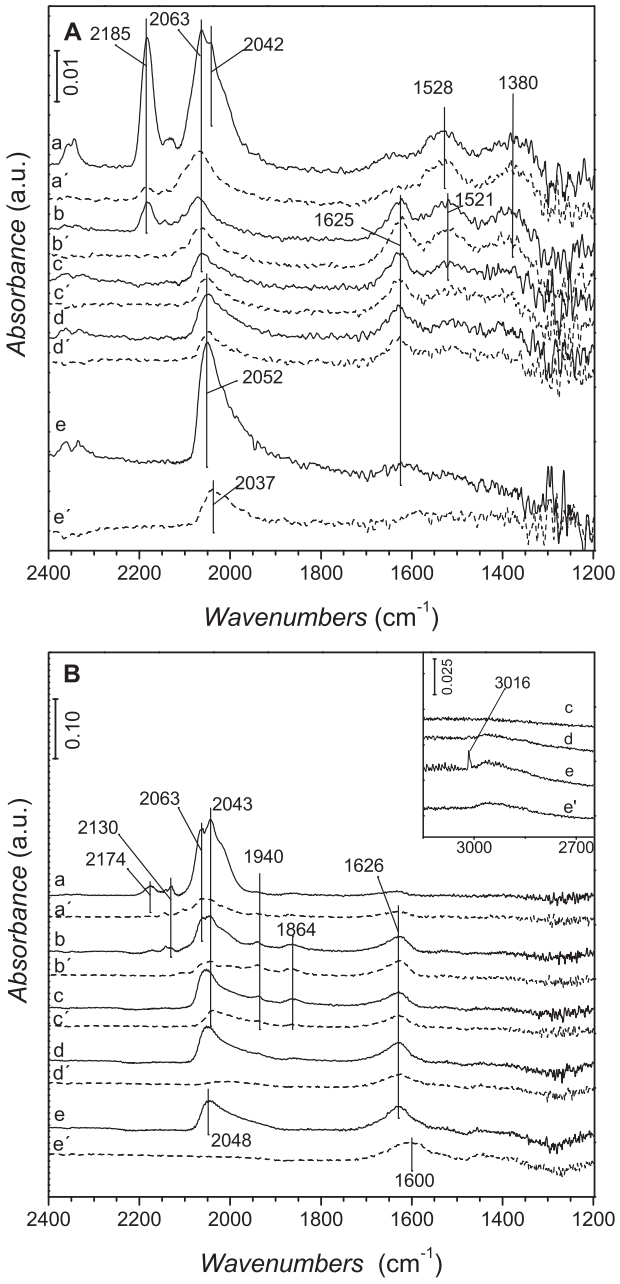

Fig. 3. *In situ* DRIFTS of Co,Pt/Co,Al-EFW (Co:Al = 1:1) under standard conditions (cf. Fig. 1). Inset: enlarged portions of spectra c, d, e and e′.

μ_3-bridging carbonyls, these may be assigned as follows. The 2131 and 2044 cm^{-1} bands are characteristic of $Co(CO)_2$ units (there is no evidence for the presence of $Co(CO)_3$ or $Co(CO)_4$ units); they have been observed on alumina matrices only at low temperatures and high pressures [31]. The band at 2066 cm^{-1} is also characteristic of Co(CO) bonding, but this time assignable to a 'tilted' Co–CO unit having a Co–C–O angle $\ll 180°$ [35]. By 100 °C, this system of bands is no longer present, being replaced by a single band at 2107 cm^{-1}, which itself then shifts to 2105 cm^{-1} (with the simultaneous appearance of a weak band at 2145 cm^{-1}) by 200 °C. The implication is that at 200 °C a Co(CO) unit bonding to the aluminosilicate sheet of the PILC is present, that this is the only Co(CO) after reaction to Co-alkyls and also (given its ready removal after He flushing) it is a weak, transient bond (Fig. 2B).

We can now compare both with the DRIFTS of Co,Pt/Co,Al-EFW, i.e. as for the Co,Al-EFW catalyst but which was ion exchanged with Co^{2+} and impregnated with Pt^{2+}. Bands at 2043 cm^{-1} and 2063 cm^{-1} in the 33%CO/H_2 stream (Fig. 3B) are in common with those for Co,Al-EFW under the same conditions the former being again assigned to linear Co(CO). The band at 2066 cm^{-1} may instead be ascribed to various causes, as pointed out by others: (i) increase in reduced Co species, (ii) cobalt surface reconstruction and (iii) presence of a hydrocarbonyl HCo(CO) species [31,33]. There is no spectral evidence (including DRS) for i and ii, whereas in both Co,Pt/Co-Al-EFW and the (non-Co substituted) Co,Al-EFW the 2043 cm^{-1} band is associated with appearance of ν(C–H) peaks at 2800–3000 cm^{-1} after 240 °C. Albeit unclear, they appear to differ and for both are more structured than expected (at 3015 cm^{-1}) for CH_4 alone. We conclude that iii is indeed the case, an HCo(CO) intermediate having previously been observed by others in similar conditions. Indeed, Kadinov et al. [31] concluded that formation of HCo(CO) is actually a *requisite* step in the overall reaction between CO and co-adsorbed H_2. In Co,Al-EFW this band is no longer present after heating to 100 °C and flushing with He (Fig. 2B b′), being replaced by a band at 2105 cm^{-1}, which in turn is accompanied by a further weak peak at 2145 cm^{-1} after raising the temperature to 200 °C. No bands are seen in the 1800–2400 cm^{-1} region after He flushing at the same temperature. The weak peak at 2105 cm^{-1} can be ascribed to carbonyl, bound to the aluminosilicate sheet.

Co,Pt/Co,Al-EFW shows a very different behaviour; the bridging CO band at 1940 cm^{-1} is weaker and now accompanied between 100 and 200 °C by an (again transient) band at 1864 cm^{-1}, also probably due to bridged CO. More importantly, the HCo(CO) peak (shifted to 2048 cm^{-1}) becomes prominent at 200 °C and appearing and disappearing with reaction/He flush (Fig. 3B, c, d′, e′). This provides strong evidence that it is involved as a weakly bonded (and hence transient) bridging moiety between the two Co ions. In addition, that Co,Al-EFW shows no evidence for the presence of the Co-HCO diagnostic peak not only confirms that the peak is not mis-assigned, but also underlines that Pt atoms on supported cobalt clusters provide the H atoms without forming observable Pt–Pt bonds (in agreement with Ref. [7]).

3.3.2. Bonding hydrocarbon region

The experimental conditions adopted (especially ambient pressure) are more suited for probing early stages of the reaction rather than CH chain propagation, this region is little developed (presumably also due to the applied relatively short time on stream). Under 33%CO/H_2 flow 15%Co/0.5%Pt/γ-Al_2O_3 shows a series of (at least) 4 peaks, at 2854, 2905, 2925, 2950 which grow in only from 200 °C (Fig. 1B inset).

The CH vibrations for Co,Al-EFW are different. In 33%CO/H_2, they appear only at >240 °C: At 280 °C two indistinct bands are apparent at 3014 and 2936 cm^{-1} (Fig. 2B inset).

3.3.3. Bonded oxygenates

We now come to the 1200–1800 cm^{-1} region, which is diagnostic for the formation of acetates, formates, carboxylates, etc. In the 3% CO regime, 15%Co,0.5%Pt/γ-alumina shows three clear bands, at 1230, 1435 and 1656 cm^{-1} (Fig. 1A), which can be assigned as bicarbonate, $\nu_s(CO_2)$ and $\nu_a(CO_2)$ vibrations [36].

Under 33% CO/H_2, the 1229, 1433, 1650 cm^{-1} series of bands (Fig. 1B) are present for bicarbonate, δ(COH), $\nu_s(CO_2)$ and $\nu_a(CO_2)$ vibrations at 30 °C, which are virtually absent at 200 °C, to be replaced by formate [32,37] or carboxylate [35] $\nu_a(CO_2)$ and $\nu_s(CO_2)$ vibrations at 1593 and 1392 cm^{-1}, respectively, and at 280 °C the two bands of unidentate carbonate at 1452 and 1373 cm^{-1} [32].

Bands in this region for Co,Al-EFW and Co,Pt/Co,Al-EFW are very different (see Figs. 2 and 3). The two final low-frequency bands at 1602 cm^{-1} and 1392 cm^{-1} (Fig. 2B) are assignable to formate $\nu_a(CO_2)$ and $\nu_s(CO_2)$ vibrations, respectively [35,37]. In Co,Pt/Co,Al-

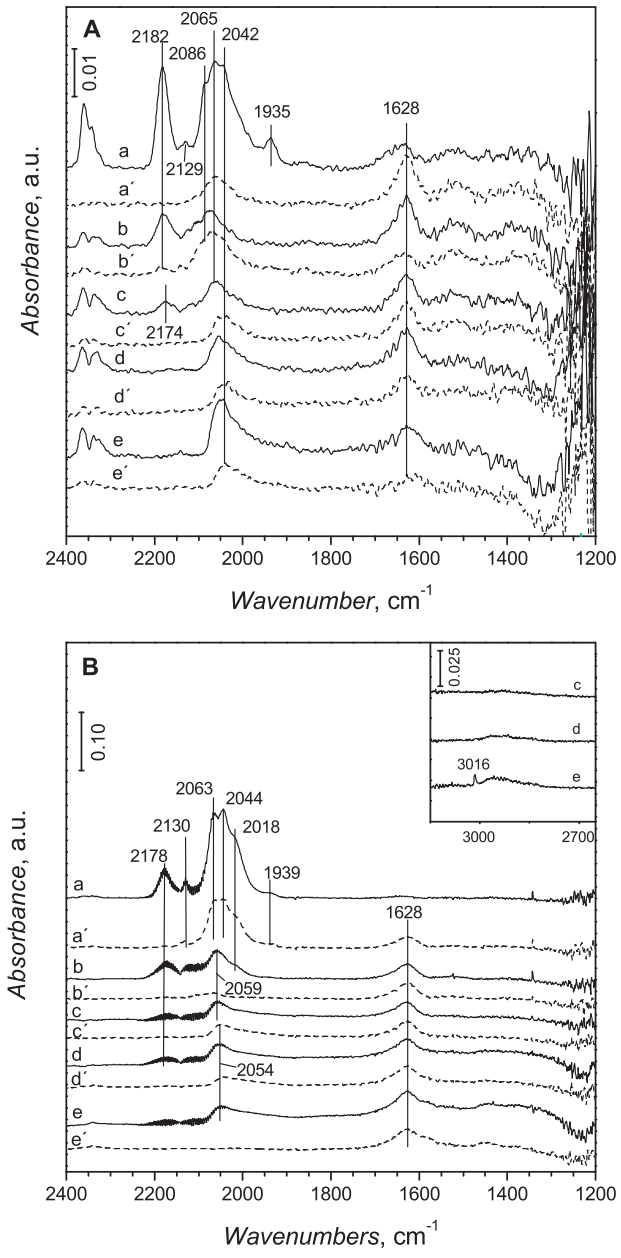

Fig. 4. *In situ* DRIFTS of Co,Pt/Co,Al-B4 (Co:Al = 1:10) under standard conditions (cf. Fig. 1). Inset: enlarged portions of spectra c, d and e.

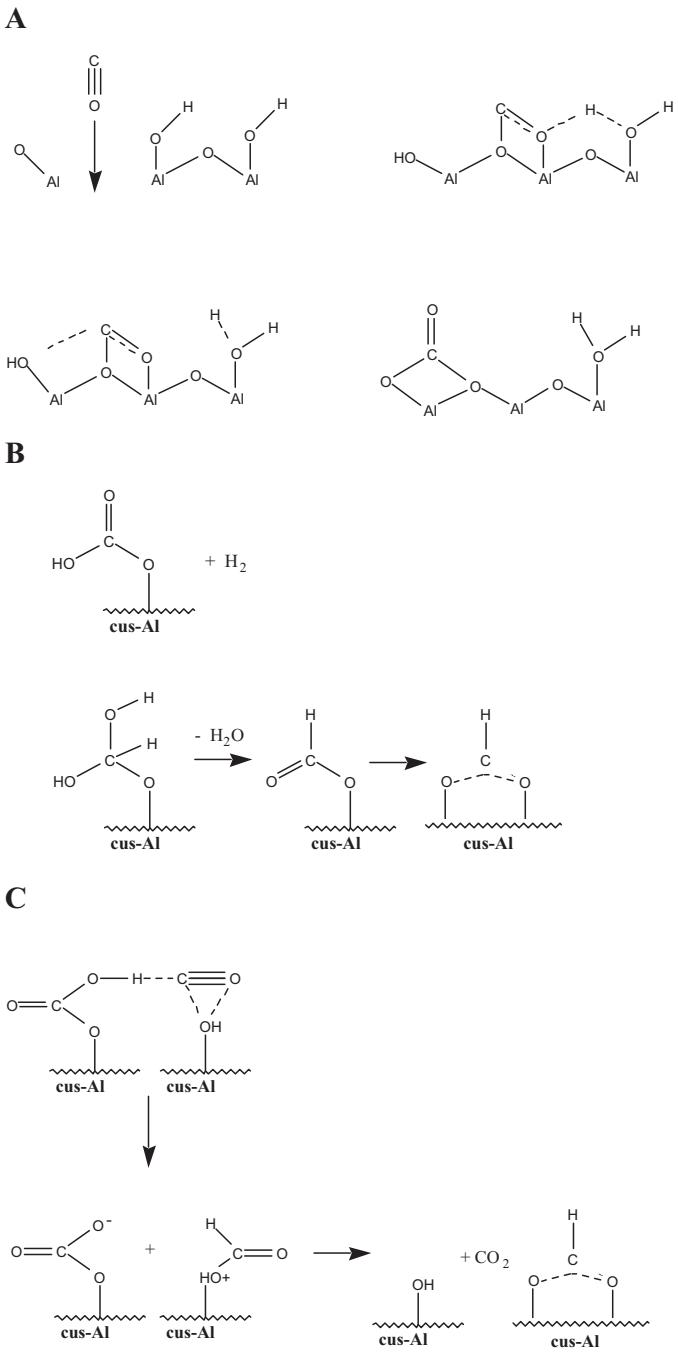

Fig. 5. (A) Scission of CO to give surface carbides in the FTS according to Ref. [40]; (B) proposed early reaction stages involving oxygenated intermediates for oxide-supported Co,Pt-catalyst.

EFW, however, under 3%CO/He flow bands appearing at 1528 cm^{-1} and 1380 cm^{-1} (Fig. 3A) can be assigned to ν_a(COO) and ν_s(COO) respectively of bidentate carbonate. They decrease in intensity with temperature increase. The formation of carbonate is presumably due to the fact that at this low coverage and in the absence of H_2, Co^{2+} is mainly present (as also indicated by the band at 2185 cm^{-1}). Conversely, formate alone is produced under a 33%CO/H_2 flow (Figs. 1B and 2B).

The appearance of the δ(H_2O) band near to 1630 cm^{-1} indicates that part of the formed water remained adsorbed (Figs. 2–4).

3.4. Active sites and mechanisms

From the above, we suggest that the Co-HCO bridges to the second Co, as shown in Fig. 5B; being labile, this rationalises the behaviour found in Figs. 3 and 4. We recall that bonding between metallic Co and CO involves electron transfer from the CO(5σ) orbital into the empty metal bands (σ donation) and simultaneous electron transfer from Co occupied bands into the CO ($2\pi^*$) orbitals (i.e. π back-donation) [19]. Presumably, a 'redox bridge' is formed by the latter interacting with Co 3*d* orbitals. (It is unlikely that the linear CoCO are responsible, since Co–C bonds are known to be strong.)

Conversely, without H_2 (Fig. 5B) Co-HCO is not formed and at ambient temperature carbonate formation occurs *via* the reaction pathway proposed by Föttinger et al. [38] (Fig. 6A) on the basis of isotope experiments. If hydrogen is not present the simultaneous formation of formate as the temperature increases must be *via* a concerted acid–base interaction with CO bonded to Al-OH groups

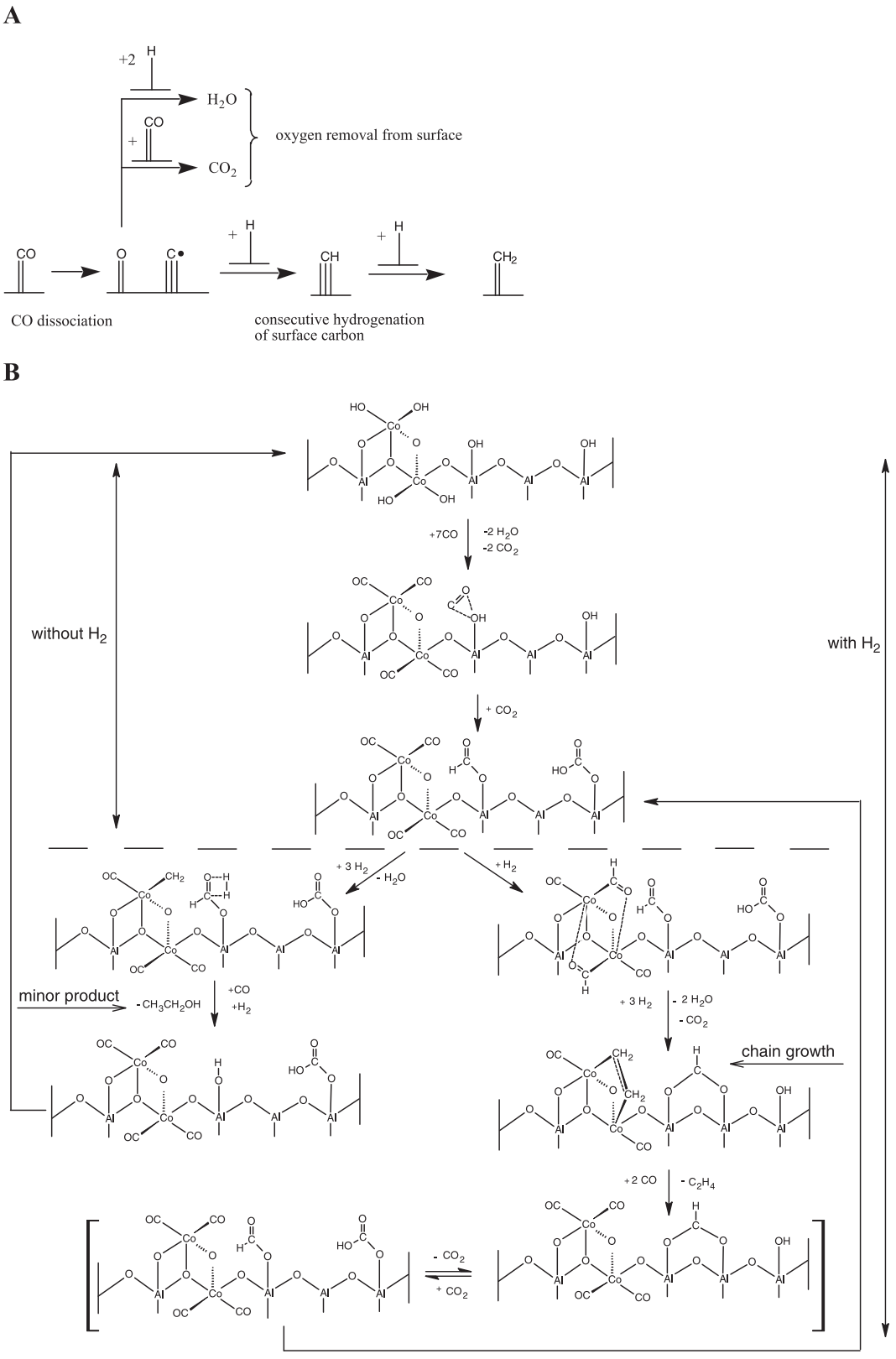

Fig. 6. (A) Carbonate formation on alumina according to Ref. [38], (B) formate formation *via* direct reduction of HCO_3^{2-} by H_2, (C) as for B, from CO and HCO_3^{2-} *via* concerted acid–base reaction [36]. Cus-Al means coordinatively unsaturated surface Al sites.

of the support. This is supported by both the enhancement in ν(OH) of the associated OH– groups and, in particular, the fact that they are labile. Such a mechanism has been put forward by Iordan et al. [36] and is shown in Fig. 6B and C.

The beidellite has a structure differs from that of montmorillonite in having tetrahedral [AlO_4] units in the sheet rather than octahedral [AlO_6] ones. Nevertheless, the DRIFTS are very similar, a further indication that active site is indeed located on the

alumina pillar. Conversely, the significantly different behaviour of 15%Co,0.5%Pt/γ-Al_2O_3 is presumably due to differences in the orientation of the binuclear active site with respect to Al-OH groups. As a final point, we recall that the Co–C=O groups are – in fact – tilted, so that very small changes in the latter cause large changes in reaction route and outcome. Since the precise surface structure in the alumina pillar of PILCs is unknown (it is γ-alumina like in natural clays) so this crucial point, i.e., the "dynamic nature" of Co centres in FTS catalysts [39] remains speculative.

The current generally accepted mechanism is shown in Fig. 5A. CO first dissociates on the surface giving rise to carbides [40] followed by hydrogenation of surface carbon to CH_x surface species. A variant is one in which polymer chain carriers are surface alkenyl rather than alkyl species, proposed by Maitlis and coworkers [41] on the basis of organometallic complex model studies. Also popular is the suggestion that oxygenates are formed by a reaction sequence in which a methyl first forms on the metal surface, which then migrates onto a surface carbonyl to form a surface acetyl [42]. Unfortunately, neither can rationalise either product variations or the variations in oxygenates uncovered by the DRIFTS. Indeed, no current mechanism answers the crucial questions underpinning the overall mechanism. These are: (i) is the H_2 added to the adsorbed CO first, therefore forming oxygen-containing intermediates, or (ii) does CO bond scission come first, hence giving rise to hydrocarbon intermediates? The current early-stage mechanism assumes that (ii) is involved, i.e. leading to surface carbides, as in Fig. 5A. However, all the DRIFTS show *no evidence* for surface carbide formation and also show that the oxygenates change according to experimental conditions, which points to involvement of (i). Particularly strong support for this is the formation of CO_3^{2-} in 15%Co,0.5%Pt/γ-alumina in the absence of hydrogen neatly supporting Iordan et al.'s acid–base scheme of Ref. [36], which as crucial intermediate involves O_2CO–H···CO H-bonds. We suggest that all is mediated by the geometry requirements of bridging Co(CHO)Co with CO HOMO(σ) + OH HOMO (lone pair) in the acid–base case and with the H_2 HOMO + LUMO orbitals in that of direct H_2 reduction of CO. Both ultimately depend on redox shuttling in the $[Co_2O_2]$ unit; although speculative, this final suggestion at least rationalises the differing temperatures at which oxygenate production kicks in (see Figs. 1–4 and 5B). In other words, CO scission probably proceeds concurrently with hydrocarbon production, as is also supported by formation of a Co-HCO moiety as reaction proceeds. Fig. 5B incorporates the formation mechanism of the oxygenate species.

The surface bond methylidene [CH_2(s)] may transform to methylidene radical [$^{\bullet}CH_2$(s)]. The $^{\bullet}CH_2$(s) radicals can couple to ethylidene and ethylidene radicals [$^{\bullet}C_2H_4$(s)]. The coupling of radicals or their reaction with gas phase hydrocarbons result in carbon chains. The MS detected in the effluent gas hydrocarbon fragments which indeed confirms this.

4. Conclusions

A detailed *in situ* DRIFTS study, backed up by optical spectra (as DRS) of an alumina-pillared montmorillonite (Co,Al-EFW) and its beidellite analogue (Co,Al-B4) has been carried out and compared with that for a commercial-type 15%Co,0.5%Pt/γ-Al_2O_3. The DRS provide evidence that Co–O–Co or Co-μO_2-Co units are present in all three cases. For the Co-PILCs, the DRIFTS point to the presence of a labile Co-HCO moiety bridging the binuclear Co units in the transition state, i.e. the H_2 adds to the adsorbed CO first. This contrasts with the previous assumption that CO bond scission occurs first, to give surface carbides. The DRIFTS also support formation of surface oxygenates (acetate, formate, etc.) *via* a concerted mechanism between the binuclear Co unit and surface Al-OH groups. The oxygenate formed varies depending on the presence or otherwise of H_2, thus confirming that oxygenated intermediate (i.e. Co-HCO) formation occurs, rather than surface carbide formation.

Further structural probing (*via* XAFS and isotope substitution) of the catalysts is underway to provide direct structural support for the active site(s) proposed and ^{18}O isotope studies to more closely define the transition state geometries involved.

Acknowledgements

We thank the Inside-pores network (UC contract: 500895) and the Hungarian Scientific Research Fund (OTKA No. 69052) for financial assistance. Authors' cooperation was supported by the Italian National Research Council (CNR), and the Hungarian Academy of Sciences (HAS).

Appendix A. Supplementary data

Supplementary data associated with this article can be found, in the online version, at doi:10.1016/j.molcata.2010.09.014.

References

[1] B.H. Davis, M.L. Occelli (Eds.), Fischer–Tropsch Synthesis, Catalysts and Catalysis, vol. 163 of Studies in Surface Science and Catalysis, Elsevier, Amsterdam, 2006.
[2] B.H. Davies, Catal. Today 141 (2008) 25–33.
[3] F. Morales, B.M. Weckhuysen, Catal. R. Soc. Chem. 19 (2006) 1–40.
[4] N.O. Elbashir, P. Dutta, A. Manivannan, M.S. Seehra, C.B. Roberts, Appl. Catal. A: Gen. 285 (2005) 169–180.
[5] A.Y. Khodakov, J. Lynch, D. Bazin, B. Rebours, N. Zanier, B. Moisson, P. Chaumette, J. Catal. 168 (1997) 16–25.
[6] G.L. Bezemer, J.H. Bitter, H.P.C.E. Kuipers, H. Oosterbeek, J.E. Holewijn, X. Xu, F. Kapteijn, A.J. van Dillen, K.P. de Jong, J. Am. Chem. Soc. 128 (2006) 3956–3964.
[7] G. Jacobs, J.A. Chaney, P.M. Patterson, T.K. Das, J.C. Maillot, B.H. Davis, J. Synchr. Rad. 11 (2004) 414–422.
[8] J. Barrault, C. Zivkov, F. Bergaya, L. Gatineau, N. Hassoun, H. Van Damme, D. Mari, Chem. Commun. (1988) 1403–1404.
[9] A. De Stefanis, A.A.G. Tomlinson, Catal. Today 114 (2006) 126–141.
[10] S.-M. Kim, Y.-J. Lee, K.-W. Jun, J.-Y. Park, H.S. Potdar, Mater. Chem. Phys. 104 (2007) 56–61.
[11] F. Lónyi, J. Valyon, L. Gutierrez, M.A. Ulla, E.A. Lombardo, Appl. Catal. B: Environ. 73 (2007) 1–10.
[12] M. LoJacono, A. Cimino, G.C.A. Schuit, Gazz. Chim. Ital. 103 (1973) 1281–1295.
[13] C. Ferragina, A. La Ginestra, M.A. Massucci, P. Patrono, A.A.G. Tomlinson, J. Phys. Chem. 89 (1985) 4762–4769.
[14] J.-M. Comets, L. Kevan, J. Phys. Chem. 97 (1993) 12004–12007.
[15] A. Bensalem, B.M. Weckhuysen, R.A. Schoonheydt, J. Phys. Chem. B 101 (1997) 2824–2829.
[16] W.-Y. Lin, H. Frei, J. Phys. Chem. B 109 (2005) 4929–4935.
[17] D. Pietrogiacomi, S. Tuti, M.C. Campa, V. Indovina, Appl. Catal. B 28 (2000) 43–54.
[18] Y. Yamasaki, M. Matsuoka, M. Anpo, Catal. Lett. 91 (1–2) (2003) 111–113.
[19] A.Y. Khodakov, W. Chu, P. Fongarland, Chem. Rev. 107 (2007) 1692–1744, and refs therein.
[20] J. Rathousky, A. Zukal, A. Lapidus, A. Krylova, Appl. Catal. 79 (1991) 167–180.
[21] R.L. Chin, D.M. Hercules, J. Phys. Chem. 86 (1982) 360–367.
[22] H-Ch. Tung, Ch-T. Yeh, Ch-T. Hong, J. Catal. 122 (1990) 211–216.
[23] H.C. Yao, M. Shelef, J. Phys. Chem. 78 (1974) 2490–2496.
[24] A.A.G. Tomlinson, J. Por. Mater. 5 (1998) 259–274.
[25] A. Clearfield, M. Kuchenmeister, in: T. Bein (Ed.), Supramolecular Architecture, vol. 499 of ACS Symposium Series, ACS, Washington, 1992 (chap. 10).
[26] I. Palinko, A. Molnar, J.B. Nagy, J.C. Bertrand, K. Lazar, J. Valyon, I. Kiricsi, J. Chem. Soc., Faraday Trans. 93 (1997) 1591–1599.
[27] J.B. Nagy, J.-C. Bertrand, I. Palinko, I. Kiricsi, J. Chem. Soc. Chem. Commun. (1995) 2269–2270.
[28] A. De Stefanis, M. Dondi, G. Perez, A.A.G. Tomlinson, Chemosphere 41 (8) (2000) 1161–1165, and refs therein.
[29] G. Busca, R. Guidetti, V. Lorenzelli, J. Chem. Soc., Faraday Trans. 86 (1990) 989–994.
[30] L.E.S. Rygh, C.J. Nielsen, J. Catal. 194 (2000) 401–409.
[31] G. Kadinov, Ch. Bonev, S. Todorova, A. Palazov, J. Chem. Soc., Faraday Trans. 94 (1998) 3027–3031.
[32] G.R. Fredriksen, E.A. Blekkan, D. Schanke, A. Holmen, Ber. Bunsenges. Phys. Chem. 97 (1993) 308–312.
[33] L.E.S. Rygh, O.H. Ellestad, P. Klaeboe, C.J. Nielsen, J. Phys. Chem. Chem. Phys. 2 (2000) 1835–1846.
[34] V. Matsouka, M. Kansolakis, R.M. Lambert, I.V. Yentekakis, Appl. Catal. B: Environ. 84 (2008) 715–722.

[35] A.A. Khassin, T.M. Yurieva, V.V. Kaichev, V.I. Bukhtiyarov, A.A. Budneva, E.A. Paukshtis, V.N. Parmon, J. Mol. Catal. A 175 (2001) 189–204.
[36] A. Iordan, M.I. Zaki, Z.C. Kappenstein, Phys. Chem. Chem. Phys. 6 (2004) 2502–2512.
[37] C.G. Visconti, L. Lietti, E. Tronconi, P. Forzatti, R. Zennaro, E. Finocchio, Appl. Catal. A: Gen. 355 (2009) 61–68.
[38] K. Föttinger, R. Schlögl, G. Rupprechter, Chem. Commun. (2008) 320–322.
[39] H. Schulz, G. Schaub, M. Claeys, T. Riedel, Appl. Catal. A: Gen. 186 (1999) 215–227.
[40] S.B. Ndlovu, N.S. Phala, M. Hearshaw-Timme, P. Beagly, J.R. Moss, M. Claeys, E. van Steen, Catal. Today 71 (2002) 343–349.
[41] H.C. Long, M.L. Turner, P. Fornasiero, J. Kašpar, M. Graziani, P.M. Maitlis, J. Catal. 167 (1997) 172–179.
[42] M.J. Overett, R.O. Hill, J.R. Moss, Coord. Chem. Rev. 206-207 (2000) 581–605.